Continuous dynamical decoupling magnetometry

Masashi Hirose,* Clarice D. Aiello,* and Paola Cappellaro†
Nuclear Science and Engineering Department and Research Laboratory of Electronics, Massachusetts Institute of Technology, Cambridge, Massachusetts 02139, USA
(Received 24 July 2012; published 20 December 2012)

Solid-state qubits hold the promise to achieve an unmatched combination of sensitivity and spatial resolution. To achieve their potential, the qubits need, however, to be shielded from the deleterious effects of the environment. While dynamical decoupling techniques can improve the coherence time, they impose a compromise between sensitivity and the frequency range of the field to be measured. Moreover, the performance of pulse sequences is ultimately limited by control bounds and errors. Here we analyze a versatile alternative based on continuous driving. We find that continuous dynamical decoupling schemes can be used for ac magnetometry, providing similar frequency constraints on the ac field and improved sensitivity for some noise regimes. In addition, the flexibility of phase and amplitude modulation could yield superior robustness to driving errors and a better adaptability to external experimental scenarios.

DOI: 10.1103/PhysRevA.86.062320 PACS number(s): 03.67.−a, 07.55.Ge, 76.30.Mi, 76.60.Lz

I. INTRODUCTION

Solid-state qubits have emerged as promising quantum sensors, as they can be fabricated in small volumes and brought close to the field to be detected. Notably, nitrogen-vacancy (NV) centers in nanocrystals of diamond [1] have been applied for high-sensitivity detection of magnetic [2–4] and electric fields [5] and could be used either as nanoscale scanning tips [6] or even *in vivo* due to their small dimensions and low cytotoxicity [7]. Unfortunately, solid-state qubits are also sensitive probes of their environmental noise [8–10] and this leads to rapid signal decay, which limits the sensor interrogation time and thus its sensitivity. Dynamical decoupling (DD) methods [11–16] have been adopted to prolong the coherence time of the sensor qubits [2,9,17–19]. Although DD techniques prevent measuring constant dc fields, they provide superior sensitivity to oscillating ac fields, as they can increase the sensor coherence time by orders of magnitude. The sensitivity is maximized by carefully matching the decoupling period to the ac field; conversely, one can study the response of a decoupling scheme to fields of various frequencies, thus mapping out their bandwidth. Still, the refocusing power of pulsed DD techniques is ultimately limited by pulse errors and bounds in the driving power. Here we investigate an alternative strategy, based on continuous dynamical decoupling (CoDD), that has the potential to overcome these limitations.

We consider the problem of measuring a small external field, coupled to the sensor by the Hamiltonian $\mathcal{H}_b = \gamma b(t) S_z$, where S_z is the spin operator of the quantum sensor. For example, $b(t)$ can be an external magnetic field and γ the spin's gyromagnetic ratio. The figure of merit for a quantum sensor is the smallest field $\delta b_{\min}$ that can be read out during a total time $\mathbf{t}$, that is, the sensitivity $\eta = \delta b_{\min}\sqrt{\mathbf{t}}$. We use this metric to compare pulsed and continuous DD schemes and show how CoDD can offer an advantage for some noise regimes. Specifically, we consider two CoDD schemes, Rabi driving [either constant continuous driving (C) or spin locking (S) [20]] and rotary echo (RE) [21–23], as their periodicity allows an easier use for ac magnetometry (see Fig. 1); we further compare these schemes to the simplest pulsed DD scheme, periodic dynamical decoupling (PDD).

II. SCHEME

The principle of DD schemes rests on the spin echo sequence, which refocuses unwanted phase accumulation due to a slow bath by reversing the system evolution with control pulses. More complex DD sequences can in principle extend the coherence time indefinitely, by increasing the number of pulses. In practice, however, a large number of imperfect, finite-width pulses provokes the accumulation of error and degrades DD performance [14,24,25]. CoDD has been first introduced in the context of NMR to mitigate pulse errors [26,27] and it has then led to many schemes, such as composite pulses [28,29], dynamically corrected gates [30], and optimized modulations [31,32]. In general, phase and amplitude modulation of the continuous driving allows great flexibility and CoDD can achieve high decoupling power [33].

As an example, we compute the signal and sensitivity of ac magnetometry under RE, but similar derivations apply for the other schemes. The RE sequence consists of a continuous on-resonance driving field of constant amplitude Ω and phase inverted at periodic intervals (see Fig. 1). RE is parametrized by the angle $\vartheta = \Omega T/2$, where T is the sequence period. While RE has been specifically designed to refocus errors in the driving field, for $\vartheta = 2\pi k$ the sequence also refocuses dephasing noise, with performance depending on both k and the Rabi frequency. We consider the evolution of a sensor qubit under a sequence of $2\pi k$ RE and in the presence of an external ac magnetic field of frequency ω whose magnitude b is to be sensed

$$\mathcal{H}(t) = \Omega h^{sw}(t) S_x + \gamma b \cos(\omega t + \varphi) S_z, \tag{1}$$

where $h^{sw}(t)$ is the square wave of period $T = 4\pi k/\Omega$. In the toggling frame of the driving field, the Hamiltonian becomes

$$\widetilde{\mathcal{H}}(t) = \frac{\gamma b \cos(\omega t + \varphi)}{2}[\cos(\Omega t) S_z - h^{sw}(t) \sin(\Omega t) S_y]. \tag{2}$$

*These authors contributed equally to this work.
†pcappell@mit.edu

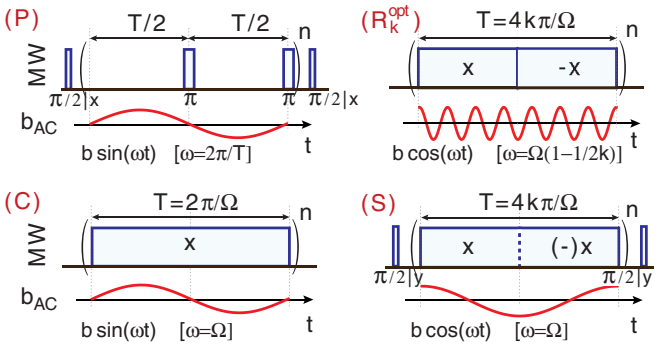

FIG. 1. (Color online) Pulse sequences for four ac magnetometry schemes: PDD (P), constant driving (C), RE with optimal frequency (R_k^{opt}), and spin locking (S). Blue boxes represent microwave driving, with phase (x and y) as indicated.

We consider only the cases where $\varphi = 0$ and $\omega T = 2m\pi$, with m an odd integer, since as we show below this yields good sensitivities. Under this assumption $\tilde{\mathcal{H}}(t)$ is periodic and for small fields b the evolution operator can be well approximated from a first-order average Hamiltonian over the period T, $\overline{\mathcal{H}} \approx \frac{1}{T}\int_0^T \tilde{\mathcal{H}}(t)dt = \gamma \overline{b}\, S_y$. The phase acquired during the evolution is thus linear in the magnetic field b to be measured. We note that this effect is true also for other RE angles ϑ; indeed, while under a continuous irradiation (C) the magnetic field contributes only to second order to the acquired phase, here the phase alternation of the driving field refocuses the effect of Rabi oscillation, enhancing the contribution of the magnetic field. Thus, the sensitivity of RE is superior to that of the constant modulation and comparable to that of PDD (or Ramsey for $\vartheta \neq 2k\pi$ [22]).

If the period of the magnetic field and the RE coincide ($m = 1$), we define $\omega_{\text{low}} = \frac{\Omega}{2k}$, which, for a fixed Ω, is easily adjustable by changing the echo angle $2\pi k$. Setting instead $m = (2k-1)$, we define $\omega_{\text{opt}} = \frac{\Omega(2k-1)}{2k}$, which yields $\overline{b} = 4bk/[\pi(4k-1)]$ and attains the best sensitivity of the method. The sensitivity, obtained as $\eta(t) = \lim_{b\to 0} \frac{\Delta\mathcal{S}}{|\frac{\partial\mathcal{S}}{\partial b}|}\sqrt{t}$, where $\mathcal{S}$ is the signal and $\Delta\mathcal{S}$ its shot-noise limited uncertainty, depends on $\overline{b}$, that is, on the averaging of the ac field over the sequence period due to the DD modulation. We compare the performance of both $2\pi k$-RE schemes to PDD (optimum $\omega = 2\pi/T$, $\varphi = \pi/2$) and a constant modulation with $\omega = \Omega$ (see Fig. 1). We obtain for the schemes considered:

$$\eta_{R_k}^{\text{opt}} = \eta\frac{4k-1}{2k} \tag{3a}$$

$$\eta_P = \eta \tag{3b}$$

$$\eta_{R_k}^{\text{low}} = \eta\frac{4k^2-1}{2k} \tag{3c}$$

$$\eta_C = \frac{4}{\pi}\eta, \tag{3d}$$

where $\eta = \frac{\pi}{2\gamma\mathcal{C}\sqrt{t}}$, with $\mathcal{C}$ a parameter capturing inefficiencies in the sensor readout [2]. Here R_k labels a $2k\pi$-RE scheme, P the PDD scheme and C the constant modulation (see Fig. 1). A fourth operating scheme can be obtained by a "spin-locking" sequence [34], where the spin is first rotated to the transverse plane before applying a driving field in the same direction; choosing $\varphi = 0$ and $\omega = \Omega$ yields the same sensitivity as for the constant modulation, $\eta_S = \eta_C$, even when the driving phase is inverted periodically.

We note that if the phase φ of the ac field is not optimized, the sensitivities are reduced by a factor $\varphi(\varphi)$, with $\varphi_P = \varphi_C = \csc(\varphi)$ and $\varphi_{R_k} = \sec\varphi$. If in addition the phase of the ac field cannot be fixed, $\varphi(\varphi) = \sqrt{2}$ when considering the average signal over many realizations.

These ideal sensitivities are degraded in the presence of noise and whenever the frequency of the ac field is not matched to the DD period. In the following we analyze these two contributions, showing that they lead to a sensitivity $\eta \to \eta\mathcal{D}(t)/W(\omega)$, where $\mathcal{D}(t)$ describes the decay under DD sequences and $W(\omega)$ is the reduction in the accumulated phase when the field frequency ω is suboptimal.

III. FREQUENCY RESPONSE

Optimal sensitivities are obtained by carefully matching the period of the DD schemes to the oscillating field. In practice, however, when field frequencies are either unknown or known to a finite precision, it is of relevance to determine the bandwidth of the scheme and the deviation from optimum sensitivities. We estimate the bandwidth by calculating the phase accumulated by the sensor over the total interrogation time $t = nT$, $\overline{B}t = \int_0^t b(t)f(t)dt$, and examining the frequency dependence of its absolute value. For PDD, the filter function is $f_P(t) = h_P^{sw}(t)$, the square wave with the period of the modulation. For continuous driving schemes such as RE and Rabi, $f(t)$ is the strength of the toggling frame Hamiltonian. In particular, $f_{R_k}(t) = h^{sw}(t)\sin(\Omega t)$ yielding the weight function $W_{R_k}(\omega) = |\overline{B}_{R_k}(\omega)|/|\overline{B}_{R_k}(\omega^{\text{opt}})|$:

$$W_{R_k}(\omega) = \frac{(4k-1)/n}{\left|(4k)^2 - \left(\frac{T\omega}{\pi}\right)^2\right|}\left|\sin(nT\omega)\tan\left(\frac{T\omega}{4}\right)\right|. \tag{4}$$

W_{R_k} has peaks (pass bands) at $\omega = 2\pi(2(k+p)-1)/T$, where p is an integer satisfying $p \geqslant 1-k$. The lowest pass band occurs for $p = 1-k$, corresponding to $\omega_{\text{low}} = \Omega/2k$. The strongest peak is for $p = 0$ at ω_{opt}. Subsequent periodic peaks are attenuated from the symmetry point $\omega = \Omega$ as $\sim\frac{\Omega^2}{|\omega^2-\Omega^2|}$. The FWHM of the optimum peak in $W_{R_k}(\omega)$ decays as $\approx\frac{7.58}{2nT}$, where $7.58 \approx$ FWHM of the squared sine function, a result common to the other DD schemes.

A similar calculation for the accumulated phase during a PDD sequence indicates the existence of peaks at $\omega = m\pi/T$, with m odd, whose intensity decays as $1/m$. This slower decay than for the RE pass bands could be beneficial if the goal is to detect fields of unknown frequencies. On the other hand, ac magnetometry under continuous driving or spin locking could be used for frequency-selective detection because $W_C(\omega)$ has a unique peak at $\omega = 2\pi/T$ with FWHM on the same order of that for RE. A comparison of the different weight functions is depicted in Fig. 2.

We note that while $W(\omega)$ describes the poor performance of DD schemes at detecting ac fields with unmatched frequencies, this property could in turn be used for frequency-selective measurements and even spectroscopy, by scanning the sequence period. While constant driving provides the best

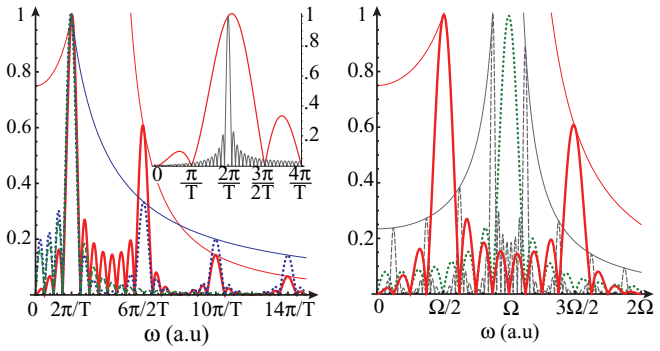

FIG. 2. (Color online) Bandwidth for ac magnetometry. We plot the weight functions $W(\omega)$ that scale the phase acquired during DD magnetometry for ac fields of frequency ω. Left: $W(\omega)$ for PDD (blue dotted), RE ($k=1$, red thick), and constant driving (green, dashed line) for $n=2$ cycles, expressing the frequency in terms of the sequence period. We also plot the envelope of the pass-band decay for PDD (blue thin) and RE (red thin), given by $\sim 1/\omega$ and $\sim\Omega^2/|\omega^2-\Omega^2|$ respectively. In the inset: we compare the main peak for $n=1$ (red, thick) and $n=10$ (gray) for RE ($k=1$) showing the reduction in bandwidth. Right: we compare $W(\omega)$ for continuous driving (green, dotted) and for RE with $k=1$ (red, thick) and $k=4$ (gray, dashed), plotting as a function of ω in units of the Rabi frequency Ω. The thin lines represent the pass-band decay envelopes for RE.

selectivity (canceling out higher octaves), RE provides more flexibility by changing both the period time and the angle $2\pi k$, which allows more uniform noise cancellation. Similarly, noise spectroscopy [8–10] can be implemented with CoDD [35] and analyzed with a method, close to the weight function, based on the filter function [15,33], which describes the DD sequence response to the noise.

IV. DECOUPLING PERFORMANCE AND ROBUSTNESS

The sensitivities in Eq. (3) are further limited by the signal decay $\mathcal{D}(t)$ under the DD sequences. The achievable sensitivity is then a compromise between the refocusing power of the sequence used and the frequency that it allows detecting (Fig. 3). While the decay for pulsed DD has been widely studied, evolution under continuous DD is more complex [36]. We can estimate the RE decay to first leading order using a cumulant expansion [37,38]. We assume a stochastic Hamiltonian, $\mathcal{H}(t)=\Omega h_k^{sw}(t)S_x+\delta(t)S_z$, where $\delta(t)$ is an Ornstein-Uhlenbeck noise with zero mean and autocorrelation function $G(\tau)=\sigma^2 e^{-\frac{\tau}{\tau_c}}$, with σ the dispersion and τ_c the correlation time. The signal decay can be calculated from the average of the superoperator

$$\langle \mathcal{S}_{R_k}\rangle = \langle\langle \widehat{0}|\mathcal{T}e^{-i\int_0^t \widehat{H}dt'}|\widehat{0}\rangle\rangle,$$

where we indicate by a hat the superoperators $\widehat{A}=A\otimes\mathbb{1}-\mathbb{1}\otimes A$, $|\widehat{0}\rangle$ is a polarized state in the Liouville space and $\mathcal{T}$ the time-ordering operator. The evolution superoperator can be approximated by the cumulants, $\langle \mathcal{T}e^{-i\int_0^t \widehat{H}dt'}\rangle \approx \exp[-(K_1+K_2+\cdots)t]$, with the first cumulant $K_1=0$ and the second given by

$$K_2=\frac{1}{2t}\int_0^t dt_1\int_0^{t_1} dt_2\,\langle \widehat{H}(t_1)\widehat{H}(t_2)\rangle_c,$$

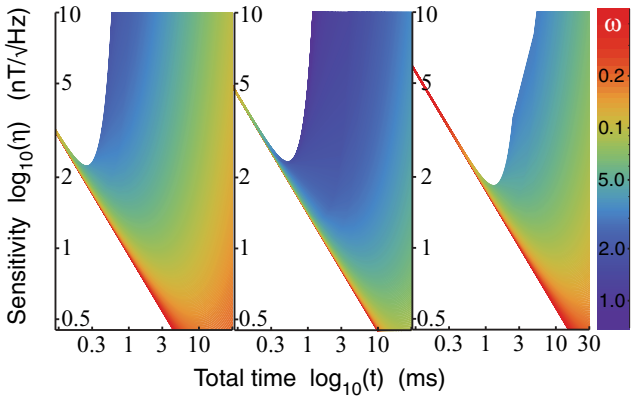

FIG. 3. (Color online) Sensitivity for ac magnetometry. We compare the magnetic field sensitivity of a single NV center for PDD (left) and RE ($k=1$ center; $k=4$ right). We assumed $T_2=500\ \mu$s under OU noise (comparable to a ^{13}C bath), yielding a decay $\propto e^{-T^3/(n^2T_2^3)}$, and a single readout with $\mathcal{C}=0.03$. A larger number of refocusing cycles (with shorter periods) achieves better sensitivity but can only detect higher frequencies, as shown by the color of the curves (right bar, MHz).

where we defined the cumulant average given by

$$\langle \widehat{H}(t_1)\widehat{H}(t_2)\rangle_c=\mathcal{T}\langle \widehat{H}(t_1)\widehat{H}(t_2)\rangle-\langle \widehat{H}(t_1)\rangle\langle \widehat{H}(t_2)\rangle.$$

In the toggling frame of the driving field, the stochastic Hamiltonian is

$$\tilde{\mathcal{H}}(t)=\delta(t)N(t)\equiv\delta(t)[\cos(\Omega t)S_z+h^{sw}(t)\sin(\Omega t)S_y].$$

Then the second cumulant for n cycles is $K_2=n\triangle+\square\sum_{j=1}^{n}(n-j)G_j$ [38], with $G_j=e^{-\frac{4k\pi j}{\Omega\tau_c}}$ and

$$\triangle=\int_0^{4k\pi/\Omega}dt_1\int_0^{t_1}dt_2\widehat{N}(t_1)\widehat{N}(t_2)G(t_1-t_2),$$
$$\square=\int_0^{4k\pi/\Omega}dt_1\int_0^{2k\pi/\Omega}dt_2\widehat{N}(t_1)\widehat{N}(t_2)G(t_1-t_2).$$

The cumulant can be written as

$$K_2=\frac{\alpha+\beta}{2}\hat{S}_z^2+\frac{\alpha-\beta}{2}\hat{S}_y^2+\frac{\sqrt{\zeta^2-\beta^2}}{2}(\hat{S}_y\hat{S}_z+\hat{S}_z\hat{S}_y)\qquad(5)$$

(see Appendix for explicit expressions), yielding the signal

$$\langle \mathcal{S}_{R_k}\rangle=\frac{1}{2}\left\{1+e^{-\alpha}\left[\cosh(\zeta)+\frac{\beta}{\zeta}\sinh(\zeta)\right]\right\}.$$

Consider for example a noise with long correlation time τ_c: In this limit, the signal decays as $\langle \mathcal{S}_{R_k}(t)\rangle=e^{-(t/T_{2R})^3/n^2}$, with $T_{2R}^{-3}=\frac{3\sigma^2}{8k^2\pi^2\tau_c}$. Numerical simulations match well with these approximate analytical results for various noise regimes. The refocusing power of RE can surpass that of pulsed schemes. Using a similar derivation as above [37,38], the decay under a PDD sequence is instead found to be $\langle \mathcal{S}_P(t)\rangle=e^{-(t/T_{2P})^3/n^2}$, with $T_{2P}^{-3}=\frac{2\sigma^2}{3\tau_c}$ for long correlation noise.

The longer coherence time under the RE sequence can be exploited either to reach a better sensitivity for a given frequency or to measure lower frequency fields at a given sensitivity, as shown in Fig. 4. The achievable improvement depends on the ratio of the effective coherence time, $\tau=T_{2R}/T_{2P}$, obtained from the two schemes. Because of the

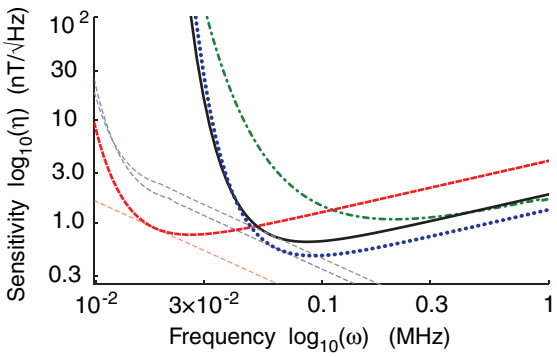

FIG. 4. (Color online) Sensitivity for ac magnetometry. We compare the achievable sensitivity for constant driving (green, dash-dotted), PDD of $n = 50$ echoes (blue, dotted) and RE (2π-RE –red, dashed– achieving the same sensitivity of PDD at a lower frequency and 8π RE –black– achieving better sensitivity than PDD at the same frequency). The chosen cycle number is experimentally achievable in the NV center system [18,39]. The period T is adjusted to match the bandwidth with the frequency of the fields. We assumed $T_2 = 500\ \mu$s under OU noise, yielding a superexponential decay $\propto e^{-T^3/(n^2T_2^3)}$, and a readout with $\mathcal{C} = 0.03$. The decay of the constant (Rabi) driving was calculated following Ref. [36] for long τ_c. In addition, the dashed, thin lines correspond to the optimal sensitivity at each frequency for each one of the sequences considered, obtained by optimizing the cycle time n (here we assumed no driving or pulse errors).

improved refocusing of RE with respect to PDD, the sensitivity can be improved for some noise regimes. In addition, RE-ac magnetometry provides the flexibility of using larger angles (larger k) to allow for longer interrogation times (Fig. 3) at lower frequencies, which could be beneficial in practical cases in combination with repeated readout schemes [22,40].

We remark that besides the decay functions obtained above in the presence of dephasing noise, other sources of decay can arise from imperfect pulses or fluctuations in the driving power. The sensitivity is thus limited not only by the coherence time, but also by pulse errors or fluctuations in the driving field. Another notable feature of the RE scheme is to improve the robustness to fluctuations of driving fields [21], which limit the sensitivity of a constant driving scheme. Thus, RE magnetometry is expected to achieve better overall sensitivities than a constant driving. In particular, RE corrects for noise varying more slowly than the RE echo time, as it has been shown experimentally [22]. Therefore, it completely refocuses the effect of static driving field errors. In contrast, simple sequences such as PDD are sensitive even to static pulse errors [25]. Although there exist many strategies to correct for these errors, such as XY4-type sequences [41] or composite pulses [29], a full comparison of the limits due to imperfection in the control fields for all these schemes is beyond the scope of this work.

V. CONCLUSION

In conclusion, we introduced a scheme for ac magnetometry based on continuous dynamical decoupling and compared its performance to pulsed DD schemes. While we focused on the simplest DD sequences, we note that more complex driving, such as composite pulses [22,29], could achieve even better refocusing of driving field instability and inhomogeneity while still providing comparable sensitivity. We further analyzed the response of ac magnetometry to fields of unknown frequencies, finding that some CoDD schemes (such as continuous driving or spin locking with alternating phases) are advantageous for spectroscopy. In addition, the flexibility of CoDD schemes in modulating both phase and amplitude of the driving field can provide practical advantages, yielding a better compromise between the DD refocusing power and the frequencies of the field to be measured.

ACKNOWLEDGMENTS

This work was supported in part by the ARO through Grant No. W911NF-11-1-0400 and by DARPA. C.D.A. acknowledges support from the Schlumberger Foundation.

APPENDIX: CUMULANT

We can calculate the time (ensemble) average of a time-ordered exponential operator by means of a cumulant expansion The first cumulant is zero since we assume a zero average as zero. The second cumulant for the RE sequence is given by Eq. (5) with

$$\alpha = \frac{\sigma^2 T^2 \tau_c e^{-\frac{nT}{\tau_c}}}{\left(e^{\frac{T}{2\tau_c}}+1\right)^2\left(16\pi^2k^2\tau_c^2+T^2\right)^2}\left\{2n\left(e^{\frac{T}{2\tau_c}}+1\right)^2 e^{\frac{nT}{\tau_c}}\left[16\pi^2k^2T\tau_c^2+64\pi^2k^2\tau_c^3\tanh\left(\frac{T}{4\tau_c}\right)+T^3\right]\right.$$
$$\left.-8\tau_c e^{\frac{(n+1)T}{2\tau_c}}\left[\left(T^2-16\pi^2k^2\tau_c^2\right)+\left(16\pi^2k^2\tau_c^2+T^2\right)\cosh\left(\frac{T}{2\tau_c}\right)\right]\sinh\left(\frac{nT}{2\tau_c}\right)\right\} \tag{A1}$$

$$\beta = -\frac{2\sigma^2 T^2 \tau_c^2 e^{-\frac{nT}{\tau_c}}}{\left(e^{\frac{T}{2\tau_c}}+1\right)^2\left(16\pi^2k^2\tau_c^2+T^2\right)^2}\left\{16\pi^2k^2\tau_c^2\left(e^{\frac{T}{2\tau_c}}-1\right)\left[e^{\frac{nT}{\tau_c}}\left((4n-1)e^{\frac{T}{2\tau_c}}+4n+1\right)+e^{\frac{T}{2\tau_c}}-1\right]+T^2\left(e^{\frac{T}{2\tau_c}}+1\right)^2\left(e^{\frac{nT}{\tau_c}}-1\right)\right\} \tag{A2}$$

$$\zeta = -\frac{2\sigma^2 T^2 \tau_c^2 e^{-\frac{nT}{\tau_c}}}{\left(e^{\frac{T}{2\tau_c}}+1\right)^2\left(16\pi^2k^2\tau_c^2+T^2\right)^2}\left\{64\pi^2k^2T^2\tau_c^2\left(e^{\frac{T}{2\tau_c}}+1\right)^4\left(e^{\frac{nT}{\tau_c}}-1\right)^2\tanh\left(\frac{T}{4\tau_c}\right)^2+\left[16\pi^2k^2\tau_c^2\left(e^{\frac{T}{2\tau_c}}-1\right)\right.\right.$$
$$\left.\left.\times\left\{e^{\frac{nT}{\tau_c}}\left[(4n-1)e^{\frac{T}{2\tau_c}}+4n+1\right]+e^{\frac{T}{2\tau_c}}-1\right\}+T^2\left(e^{\frac{T}{2\tau_c}}+1\right)^2\left(e^{\frac{nT}{\tau_c}}-1\right)\right]^2\right\}^{1/2} \tag{A3}$$

[1] F. Jelezko, I. Popa, A. Gruber, C. Tietz, J. Wrachtrup, A. Nizovtsev, and S. Kilin, Appl. Phys. Lett. **81**, 2160 (2002).
[2] J. M. Taylor, P. Cappellaro, L. Childress, L. Jiang, D. Budker, P. R. Hemmer, A. Yacoby, R. Walsworth, and M. D. Lukin, Nature Phys. **4**, 810 (2008).
[3] J. R. Maze, P. L. Stanwix, J. S. Hodges, S. Hong, J. M. Taylor, P. Cappellaro, L. Jiang, A. Zibrov, A. Yacoby, R. Walsworth, and M. D. Lukin, Nature (London) **455**, 644 (2008).
[4] G. Balasubramanian, I.-Y. Chan, R. Kolesov, M. Al-Hmoud, C. Shin, C. Kim, A. Wojcik, P. R. Hemmer, A. Krüger, F. Jelezko, and J. Wrachtrup, Nature (London) **445**, 648 (2008).
[5] F. Dolde, H. Fedder, M. W. Doherty, T. Nobauer, F. Rempp, G. Balasubramanian, T. Wolf, F. Reinhard, L. C. L. Hollenberg, F. Jelezko, and J. Wrachtrup, Nature Phys. **7**, 459 (2011).
[6] P. Maletinsky, S. Hong, M. S. Grinolds, B. Hausmann, M. D. Lukin, R. L. Walsworth, M. Loncar, and A. Yacoby, Nature Nano **7**, 320 (2012).
[7] L. P. McGuinness, Y. Yan, A. Stacey, D. A. Simpson, L. T. Hall, D. Maclaurin, S. Prawer, P. Mulvaney, J. Wrachtrup, F. Caruso, R. E. Scholten, and L. C. L. Hollenberg, Nature Nano **6**, 358 (2011).
[8] J. Bylander, S. Gustavsson, F. Yan, F. Yoshihara, K. Harrabi, G. Fitch, D. G. Cory, and W. D. Oliver, Nature Phys. **7**, 565 (2011).
[9] N. Bar-Gill, L. Pham, C. Belthangady, D. Le Sage, P. Cappellaro, J. Maze, M. Lukin, A. Yacoby, and R. Walsworth, Nature Commun. **3**, 858 (2012).
[10] K. C. Young and K. B. Whaley, Phys. Rev. A **86**, 012314 (2012).
[11] H. Y. Carr and E. M. Purcell, Phys. Rev. **94**, 630 (1954).
[12] L. Viola, E. Knill, and S. Lloyd, Phys. Rev. Lett. **82**, 2417 (1999).
[13] G. S. Uhrig, Phys. Rev. Lett. **98**, 100504 (2007).
[14] K. Khodjasteh and D. A. Lidar, Phys. Rev. A **75**, 062310 (2007).
[15] M. J. Biercuk, A. C. Doherty, and H. Uys, J. Phys. B **44**, 154002 (2011).
[16] G. A. Álvarez, A. Ajoy, X. Peng, and D. Suter, Phys. Rev. A **82**, 042306 (2010).
[17] G. de Lange, D. Ristè, V. V. Dobrovitski, and R. Hanson, Phys. Rev. Lett. **106**, 080802 (2011).
[18] L. M. Pham, N. Bar-Gill, C. Belthangady, D. Le Sage, P. Cappellaro, M. D. Lukin, A. Yacoby, and R. L. Walsworth, Phys. Rev. B **86**, 045214 (2012).
[19] S. Kotler, N. Akerman, Y. Glickman, A. Keselman, and R. Ozeri, Nature (London) **473**, 61 (2011).
[20] M. Loretz, T. Rosskopf, and C. L. Degen, arXiv:1210.1443.
[21] I. Solomon, Phys. Rev. **110**, 61 (1958).
[22] C. D. Aiello, M. Hirose, and P. Cappellaro, arXiv:1207.5868 [Nature Comm. (to be published)].
[23] A. Laraoui and C. A. Meriles, Phys. Rev. B **84**, 161403 (2011).
[24] K. Khodjasteh and D. A. Lidar, Phys. Rev. Lett. **95**, 180501 (2005).
[25] Z.-H. Wang, W. Zhang, A. M. Tyryshkin, S. A. Lyon, J. W. Ager, E. E. Haller, and V. V. Dobrovitski, Phys. Rev. B **85**, 085206 (2012).
[26] D. Burum, M. Linder, and R. R. Ernst, J. Mag. Res. **44**, 173 (1981).
[27] G. S. Boutis, P. Cappellaro, H. Cho, C. Ramanathan, and D. G. Cory, J. Mag. Res. **161**, 132 (2003).
[28] A. Shaka, J. Keeler, and R. Freeman, J. Mag. Res. **53**, 313 (1983).
[29] M. H. Levitt, Prog. Nucl. Mag. Res. Spect. **18**, 61 (1986).
[30] K. Khodjasteh and L. Viola, Phys. Rev. A **80**, 032314 (2009).
[31] N. Cody Jones, T. D. Ladd, and B. H. Fong, New J. Phys. **14**, 093045 (2012).
[32] F. F. Fanchini, J. E. M. Hornos, and R. d. J. Napolitano, Phys. Rev. A **75**, 022329 (2007).
[33] T. Green, H. Uys, and M. J. Biercuk, Phys. Rev. Lett. **109**, 020501 (2012).
[34] A. G. Redfield, Phys. Rev. **98**, 1787 (1955).
[35] S. Gustavsson, J. Bylander, F. Yan, P. Forn-Diaz, V. Bolkhovsky, D. Braje, G. Fitch, K. Harrabi, D. Lennon, J. Miloshi, P. Murphy, R. Slattery, S. Spector, B. Turek, T. Weir, P. B. Welander, F. Yoshihara, D. G. Cory, Y. Nakamura, T. P. Orlando, and W. D. Oliver, Phys. Rev. Lett. **108**, 170503 (2012).
[36] V. V. Dobrovitski, A. E. Feiguin, R. Hanson, and D. D. Awschalom, Phys. Rev. Lett. **102**, 237601 (2009).
[37] R. Kubo, J. Phys. Soc. Jpn. **17**, 1100 (1962).
[38] P. Cappellaro, J. S. Hodges, T. F. Havel, and D. G. Cory, J. Chem. Phys. **125**, 044514 (2006).
[39] C. A. Ryan, J. S. Hodges, and D. G. Cory, Phys. Rev. Lett. **105**, 200402 (2010).
[40] P. Neumann, J. Beck, M. Steiner, F. Rempp, H. Fedder, P. R. Hemmer, J. Wrachtrup, and F. Jelezko, Science **329**, 542 (2010).
[41] T. Gullion, D. B. Baker, and M. S. Conradi, J. Mag. Res. **89**, 479 (1990).